Detailed simulations of plasma-induced spectral blueshifting

S. C. Rae and K. Burnett

Department of Physics, Clarendon Laboratory, University of Oxford, Oxford OX1 3PU, United Kingdom
(Received 13 January 1992; revised manuscript received 16 March 1992)

A one-dimensional model, including pulse propagation and detailed ionization dynamics, is developed in order to calculate the spectrum of an intense femtosecond laser pulse transmitted through an atmospheric-density noble gas. The spectrum is broadened and blueshifted due to self-phase-modulation resulting from a combination of optical-field-induced ionization and collisional ionization. Different features in the spectrum can be used to indicate the relative importance of the two ionization mechanisms. The calculations are in good agreement with the recent experimental results of Wood, Siders, and Downer [Phys. Rev. Lett. **67**, 3523 (1991)], but indicate that a significant degree of defocusing occurs as a result of plasma generation. The simulations could possibly be used as a test of various theoretical models for optical-field-induced ionization.

I. INTRODUCTION

As an intense femtosecond laser pulse propagates through a gas, optical-field-induced ionization (OFI) and collisional ionization can cause a rapid increase in the electron density, and hence a decrease in the refractive index. This self-phase-modulation leads to the complementary effects of spatial defocusing and spectral broadening. The effects are markedly different to those which result from self-phase-modulation at lower intensities [1], because the polarizibility of free electrons is relatively large and the rate of ionization is a highly nonlinear function of the intensity. In addition, the ionization process is essentially irreversible on a femtosecond time scale, and as a result the spectral broadening is one sided, containing predominantly blueshifted components.

Plasma-induced self-phase-modulation was first proposed by Bloembergen [2] almost twenty years ago, and the early experiments of Yablonovitch [3] concerned plasma generation by avalanche collisional ionization using a nanosecond-pulse CO_2 laser. Corkum [4] has also observed spectral blueshifting due to collisional ionization with a high-power picosecond-pulse CO_2 laser. With the advent of high-intensity ($> 10^{15}$ W/cm^2) femtosecond-pulse lasers, however, a different class of experiments is now possible in which OFI plays a dominant role. Recent experiments by Downer and co-workers [5–8] using a dye laser producing 100-fs, 620-nm pulses at a focused intensity of up to 10^{16} W/cm^2 have shown that the initial spectrum can be blueshifted by 10–50 nm. Such a process is of fundamental interest, as it may allow the testing of various models for OFI in intense laser fields, and it may also have a practical application as a broadband spectroscopic source.

In order to understand the plasma dynamics in these experiments, and also to have confidence in predicting the behavior for different laser parameters or different focusing geometries, it is important to have a detailed model which includes not only ionization but also the propagation of the laser pulse. Simple models proposed so far have provided useful insights into the mechanisms responsible for blueshifting, and it is the purpose of this paper to expand on these and incorporate a more detailed description of the underlying physics.

II. SPECTRAL BLUESHIFTING

Plasma-induced spectral blueshifting has been analyzed in the past [3,5] using a homogeneous model, in which the plasma is described by a single value of the refractive index n. For an incident wavelength λ_0 and an interaction length L, the spectral shift is given by

$$\Delta\lambda = \frac{\lambda_0 L}{c}\frac{dn}{dt} . \tag{1}$$

Neglecting collisions, the plasma refractive index can be written $n = (1 - N_e/N_{cr})^{1/2}$, where N_e is the electron density and $N_{cr} = \epsilon_0 m_e \omega_0^2/e^2$ is the critical density. Making the reasonable assumption for gaseous densities that $N_e \ll N_{cr}$, the spectral shift can be expressed as

$$\Delta\lambda = -\frac{e^2 N_i \lambda_0^3 L}{8\pi^2 \epsilon_0 m_e c^3}\frac{dZ}{dt} , \tag{2}$$

where N_i is the ion density and Z is the degree of ionization. An estimate of the shift thus depends on an accurate calculation of the ionization rate.

A number of theoretical approaches have been developed in recent years for calculating OFI rates. These approaches generally fall into one of two regimes, distinguished by the adiabaticity parameter,

$$\gamma = (\mathscr{E}_i/2\mathscr{E}_q)^{1/2} . \tag{3}$$

Here $\mathscr{E}_i$ is the ionization potential and $\mathscr{E}_q$ is the ponderomotive or quiver energy, given by

$$\mathscr{E}_q = e^2 E_0^2/4m_e\omega_0^2 . \tag{4}$$

In the limit $\gamma \gg 1$ the ionization rate obeys a perturbative power law, but for $\gamma \lesssim 1$ a tunneling picture is more

DETAILED SIMULATIONS OF PLASMA-INDUCED SPECTRAL . . .

appropriate. The conditions of this paper correspond to the tunneling regime, and ionization rates are calculated using a generalized tunneling formula due to Ammosov, Delone, and Krainov (ADK) [9], based on earlier work by Perelomov, Popov, and Terentev [10]. The ionization rate in a static electric field E is given by

$$\mathcal{R}_{st} = \frac{\omega_{at}}{2} C_{n*}^2 \frac{\mathcal{E}_i}{\mathcal{E}_h} \frac{(2l+1)(l+|m|)!}{2^{|m|}(|m|)!(l-|m|)!}$$
$$\times \left[2 \left[\frac{\mathcal{E}_i}{\mathcal{E}_h} \right]^{3/2} \frac{E_{at}}{E} \right]^{2n*-|m|-1}$$
$$\times \exp \left[-\frac{2}{3} \left[\frac{\mathcal{E}_i}{\mathcal{E}_h} \right]^{3/2} \frac{E_{at}}{E} \right] . \qquad (5)$$

Here $\mathcal{E}_h$ is the ionization potential for hydrogen, ω_{at} and E_{at} are the atomic units for frequency and electric field, l and m are quantum numbers for the initial state, $n* = Z(\mathcal{E}_h/\mathcal{E}_i)^{1/2}$ is the effective principle quantum number, and $C_{n*} = (2e/n*)^{n*}(2\pi n*)^{-1/2}$, where e is Euler's number. Equation (5) can be averaged over an optical cycle to obtain the mean ionization rate in a sinusoidal field,

$$\mathcal{R} = \left[\frac{3}{\pi} \frac{E}{E_{at}} \left[\frac{\mathcal{E}_h}{\mathcal{E}_i} \right]^{3/2} \right]^{1/2} \mathcal{R}_{st} . \qquad (6)$$

Recent experiments by Augst et al. [11] on the production of highly charged ions using a picosecond-pulse Nd:glass laser have shown good agreement with ADK ionization rates, if a species-dependent scaling factor of order unity is included [12].

Assuming that the atoms and ions are in their ground states, and only considering sequential ionization processes, the populations of the various ionization stages can be obtained from a set of coupled first-order differential equations of the form

$$\frac{dN_k}{dt} = -\mathcal{R}_k N_k + \mathcal{R}_{k-1} N_{k-1} , \qquad (7)$$

where $\mathcal{R}_k$ is the ionization rate and N_k the population of the kth stage.

As an example, we will consider argon gas and a 100-fs full width at half maximum (FWHM) sine-squared-envelope laser pulse with a peak intensity of 10^{16} W/cm^2. Figure 1 shows the ionic populations as a function of time, obtained using cycle-averaged ionization rates from Eq. (6). During the leading edge of the pulse, the degree of ionization increases in a series of steps as the threshold intensities for successive ionization stages are reached, with corresponding peaks in dZ/dt shown in the lower half of the figure. The blueshift in this simple example can be quite large: for a gas pressure of 5 atm and an interaction length of 100 μm, the shift (in nm) from Eq. (2) is given by $\Delta\lambda = 4.5 \times 10^3 (dZ/dt)$, with dZ/dt in units of fs^{-1}. The transmitted spectrum would be expected to include a number of almost distinct blueshifted components, with a significant fraction of the pulse energy, in the trailing edge, transmitted unshifted in wavelength.
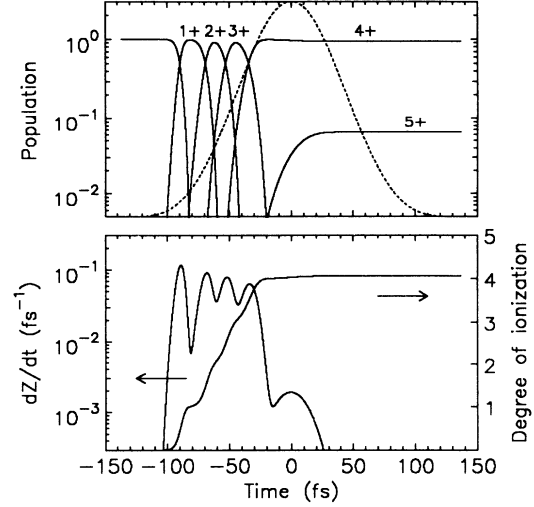

FIG. 1. Relative populations of the ionization stages of Ar for a 100-fs FWHM laser pulse, shown dotted, with peak intensity 10^{16} W/cm^2 (top). Degree of ionization and dZ/dt as functions of time (bottom).

For a refractive index which varies in space, Eq. (1) can be generalized to

$$\Delta\lambda = \frac{\lambda_0}{c} \int_0^L \frac{\partial n(x)}{\partial t} dx , \qquad (8)$$

which assumes that the total spectral shift can be broken down into a sum over independent shifts from each point in the plasma. While this may be a good approximation for long laser pulses, it breaks down when considering ionization in a femtosecond pulse, for two major reasons: (i) the expression assumes that the transit time through the medium is much less than the time scale associated with the changing refractive index; and (ii) it has been derived for monochromatic light (or a transform-limited pulse with a slowly varying envelope) and assumes that there is a single well-defined value for the shift. In practice, the initial spectrum of the pulse becomes modified in a more complicated way than a simple translation.

III. PROPAGATION MODEL

To calculate the complete spectrum, rather than just a single-valued shift, the wave equation needs to be solved for the propagation of a laser pulse through the gas, including a separate ionization rate calculation at each point. In one dimension (1D), assuming linearly polarized light propagating along the x axis, the equation to be solved is

$$\frac{\partial^2 E}{\partial x^2} - \frac{1}{c^2} \frac{\partial^2 E}{\partial t^2} - \mu_0 \frac{\partial J}{\partial t} = 0 , \qquad (9)$$

where $E = E(x,t)$ is the transverse electric field and $J = J(x,t)$ is the transverse plasma current. In a full calculation, the current would be derived from an electron distribution function,

$$J(x,t) = -e \int f_e(x,v,t)v \, dv , \qquad (10)$$

and the evolution of this distribution function would be governed by a Boltzmann equation,

$$\frac{\partial f_e}{\partial t} + v\frac{\partial f_e}{\partial r} - \frac{eE}{m_e}\frac{\partial f_e}{\partial v} = \mathcal{C}(f) + \mathcal{S}(f) ,\qquad (11)$$

where $\mathcal{S}(f)$ is a source term (from ionization) and $\mathcal{C}(f)$ is the collision integral. Here we have neglected effects due to the magnetic field, which restricts the model to the nonrelativistic regime $v_q \ll c$, where v_q is the peak quiver velocity. Thus the intensity is limited to

$$I \ll 5.5 \times 10^{18} \left[\frac{500\ \text{nm}}{\lambda_0} \right]^2 \ \text{W/cm}^2 .\qquad (12)$$

In order to make the system of equations amenable to numerical solution on a computer of moderate size, we simplify Eq. (10) by assuming that the free electrons behave coherently and can be adequately described by an average velocity $\bar{v}(x,t)$. The plasma current then becomes

$$J(x,t) = -eN_e(x,t)\bar{v}(x,t) .\qquad (13)$$

The electron density $N_e(x,t)$ is found from the solution of the ionization rate equations, and we can then use the fact that the mean electron velocity evolves according to the following equation of motion:

$$\frac{\partial \bar{v}}{\partial t} + v_{ei}\bar{v} = \frac{-eE}{m_e} .\qquad (14)$$

Here v_{ei} is the effective electron-ion collision frequency, which appears as a frictional damping term. We should emphasize that the critical phase relationship between the laser driving field and the mean velocity of the electrons is preserved by this approximation. All we are doing is ignoring the details of the electron-velocity distribution; we are still following the mean velocity as it oscillates in the field.

To ensure energy conservation during ionization, an additional ionization current J_{ioniz} is introduced, such that the Ohmic power dissipation equals the ionization energy loss,

$$EJ_{\text{ioniz}} = \sum_k \mathcal{R}_k N_k \mathcal{E}_k .\qquad (15)$$

We use an explicit finite-difference method to solve numerically the wave equation, Eq. (9), together with the coupled population equations, Eq. (7), and the electron equation of motion, Eq. (14), at each point in the plasma. The ionization rates for the population equations are calculated from Eq. (5) using the instantaneous value of the electric field.

The main effect of the simplification from the full electron distribution function to an average velocity is to neglect the above-threshold-ionization (ATI) energy of the electrons, which in any case is small compared with the ionization potentials. In addition, we generally set $v_{ei} = 0$ in Eq. (14), as the background temperature from collisional heating never becomes large enough for thermal collisional ionization to compete with OFI. At higher intensities ($I \gg 10^{16}$ W/cm^2) these approximations would need to be reconsidered; at such intense field

strengths the atoms are highly stripped and both ATI and collisional heating become important. This regime is currently of some interest in proposed recombination x-ray laser schemes, for which the plasma temperature is a crucial factor, and the application of the present model to this regime will be discussed in a separate communication [13].

IV. SIMULATION RESULTS

The blueshifted spectrum obtained from the propagation model depends on a large number of parameters: laser wavelength, peak intensity, pulse shape and duration, gas species, pressure, and interaction length. In this section we present a number of results for a 620-nm, 100-fs FWHM laser pulse with a sine-squared field envelope.

Figure 2 shows the transmitted pulse spectra for a peak intensity of 10^{16} W/cm^2 and an interaction length of 50 μm, in a number of different noble gases at 5 atm pressure. The ionization potentials decrease from neon to krypton, and this is reflected in the progressively larger blueshifts. The final degree of ionization under these conditions varies from 2.01 in neon to 4.14 in argon, and 6.01 in krypton. It is not possible to find an isolated feature associated with each ionization stage, as predicted by the homogeneous-plasma model and suggested by Fig. 1; instead the spectrum is complex and irregular. However, it is clear that the detail at large blueshifts corresponds to rapid ionization early in the leading edge of the pulse, while detail closer to the original wavelength is connected with ionization occurring more slowly across the peak of the pulse. A significant fraction of the pulse energy remains unshifted, corresponding to the trailing edge of the pulse where the ionization rate is close to zero.

The dependence of the transmitted pulse spectrum on laser intensity is shown in Fig. 3, for a 50 μm length of 5-atm argon. The maximum blueshift increases roughly proportionally with the degree of ionization, although the spectrum does not necessarily increase in complexity.

An important prediction of the simple homogeneous model, Eq. (2), is that the blueshift should scale linearly with the interaction length. Figure 4 shows that this is approximately verified by the propagation model, but
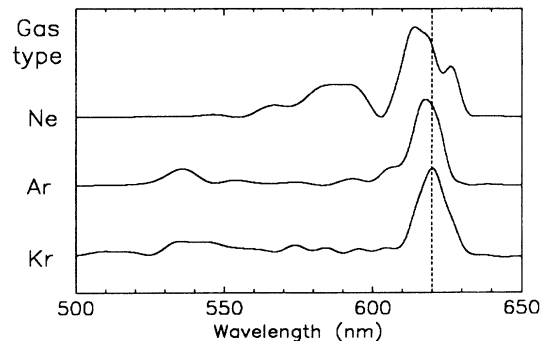

FIG. 2. Transmitted-pulse spectra for a 620-nm, 100-fs FWHM pulse with peak intensity of 10^{16} W/cm^2, and a 50 μm length of different noble gases at a pressure of 5 atm.
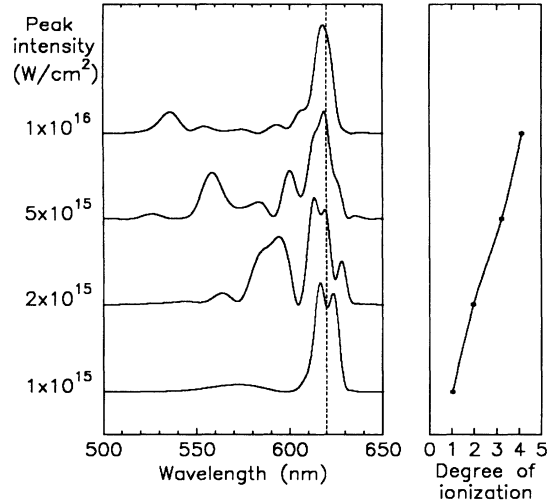
FIG. 3. Transmitted pulse spectra and final degree of ionization at different peak intensities, for a 620-nm, 100-fs FWHM pulse and 50 μm of Ar at 5 atm.

FIG. 5. Incident (left) and transmitted (right) electric field, for a 620-nm, 100-fs FWHM pulse at 5×10^{15} W/cm^2 and 100 μm of Ar at 5 atm. The peak incident field is normalized to unity.

only in the narrow sense that the maximum shift is proportional; the overall change is not simply one of expansion along the wavelength axis. The absorption due to ionization is also plotted in this figure, and it is significant that under these conditions only a very small fraction of the pulse energy is lost, even though the spectrum can be severely modified.

The detailed structure observed for large interaction lengths is partly due to amplitude as well as phase modulation. This can be seen in Fig. 5, where the incident and transmitted electric field is plotted for the case of a 100 μm length of 5-atm argon. Steplike features in the leading edge of the transmitted pulse are associated with the threshold intensities for various ionization stages, and the
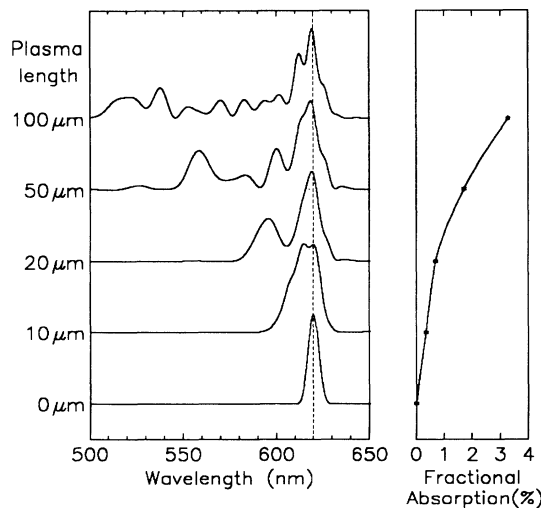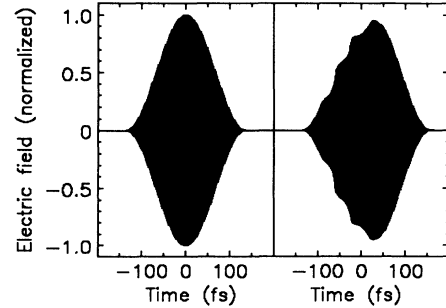

FIG. 4. Transmitted pulse spectra and fractional absorption due to ionization for different interaction lengths, with a 620-nm, 100-fs FWHM pulse at a peak intensity of 5×10^{15} W/cm^2, and Ar at 5 atm.

pulse has also been stretched in time by an amount on the order of 10%. This degree of temporal broadening, and the small fraction of pulse energy absorbed, are both features observed in related experiments [8,15].

V. COLLISIONAL IONIZATION

Although the background thermal temperature due to collisional heating is too small to lead to additional ionization, the quiver motion of the free electrons in the plasma can be sufficiently large to cause ionization by electron impact. The average quiver energy reaches 360 eV for 620-nm light at an intensity of 10^{16} W/cm^2, which is well above the ionization potentials of the first few ionization stages of the noble gases.

Collisional ionization is incorporated into the propagation model by modifying the ionization rate equations so that at each point and for each ionization stage there is an additional ionization rate,

$$\mathcal{R} = \mathcal{R}_{OFI} + N_e \bar{v} \sigma(\bar{v}) , \qquad (16)$$

where σ is the energy-dependent cross section for the appropriate species and ionization stage [14]. Energy conservation is maintained at each time step by subtracting the energy required for collisional ionization from the total kinetic energy of the free electrons.

Unlike OFI, which mainly occurs while the intensity is increasing in the leading edge of the laser pulse, collisional ionization can occur almost right across the pulse, although at a slower rate. This can be seen in Fig. 6, which shows the degree of ionization and dZ/dt in the centre of a 50-μm argon plasma, with a 100-fs laser pulse of peak intensity 10^{16} W/cm^2. Comparing this with Fig. 1, which is calculated under the same conditions but without collisional ionization, it can be seen that the final degree of ionization has been increased slightly, and that there is now a higher ionization rate over the peak of the pulse and in the trailing edge. Figure 7 shows the transmitted pulse spectra for the same conditions as previously seen in Fig. 3, but now including collisions. The overall effect on the spectrum is to blueshift the main peak by a small amount, without significantly altering the existing detail at larger shifts. The final degree of ionization is raised in
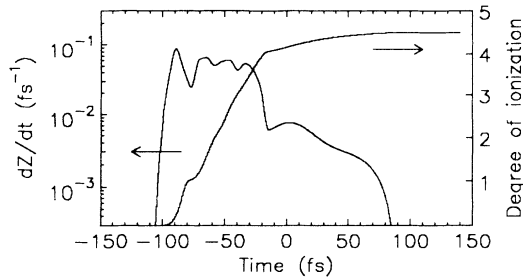
FIG. 6. Degree of ionization and dZ/dt as functions of time, in the center of a 50-μm, 5-atm Ar plasma with a 620-nm, 100-fs FWHM pulse at a peak intensity of 10^{16} W/cm^2, including collisional ionization.

each case by a similar, small amount, typically 0.2–0.3.

For comparison with experimental results, consideration must be given to intensity variations, both transverse to the direction of propagation and longitudinally through the focus. As a 1D model is not really suitable for addressing the issue of spatial behavior, we limit ourselves to taking a simple average across a transverse Gaussian intensity profile. An ideal Gaussian beam of diameter D entering a thin lens of focal length f has a confocal parameter z_c given by

$$z_c = \frac{8\lambda_0 f^2}{\pi D^2} . \tag{17}$$

In order to approximate the effect of focusing, we average a number of spectra (typically 20), calculated for an interaction length equal to z_c, over a transverse Gaussian profile. The net result of this averaging procedure is to smooth out most of the blueshifted features seen earlier into a uniform blueshifted shoulder, with collisional ion-
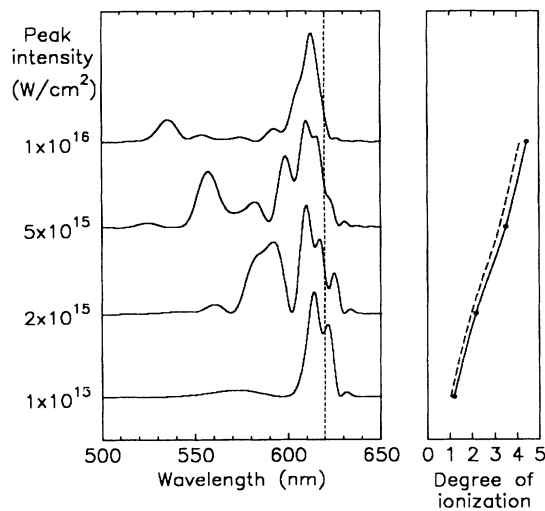

FIG. 7. Transmitted pulse spectra for the same conditions as Fig. 3, but including collisional ionization. The degree of ionization without collisions is shown as a dashed line, to emphasize the increase due to the collisional process.

ization producing a small additional blueshift of the main peak.

Figure 8 shows the averaged spectra for 5 atm of neon, argon, and krypton at several peak intensities in the range 10^{15}–10^{16} W/cm^2. We have assumed $f/5$ focusing ($z_c = 40$ μm) to allow direct comparison with the recent experimental results of Wood, Siders, and Downer [8]. The spectra for all the gases show the same basic features: a main peak blueshifted by $\lesssim 5$ nm, and a weak shoulder extending further into the blue. In krypton at a peak intensity of 10^{16} W/cm^2 this shoulder extends for some 100 nm; in neon, where the ionization potentials are higher, the extent is significantly less.

The small blueshift of the main peak is almost unchanged with intensity and is similar for the three gases. This behavior follows from a choice of wavelength, 620 nm, where the quiver energy is well matched to the ionization potentials. As the intensity increases, the atoms are stripped to higher ionization stages by OFI, but the quiver energy also increases, so that over a wide range in intensity the collisional contribution to ionization remains almost constant. The same would not necessarily be true for a different laser wavelength. This can be seen from Fig. 9, where three spectra are shown for different wavelengths but otherwise identical pulse parameters, and an interaction length in each case equal to the confocal parameter for $f/5$ focusing (16 μm for 248 nm, 40 μm for 620 nm, 51 μm for 800 nm). At 248 nm, the quiver energy is only 57 eV at 10^{16} W/cm^2 and collisional ionization is negligible; the main peak in this case
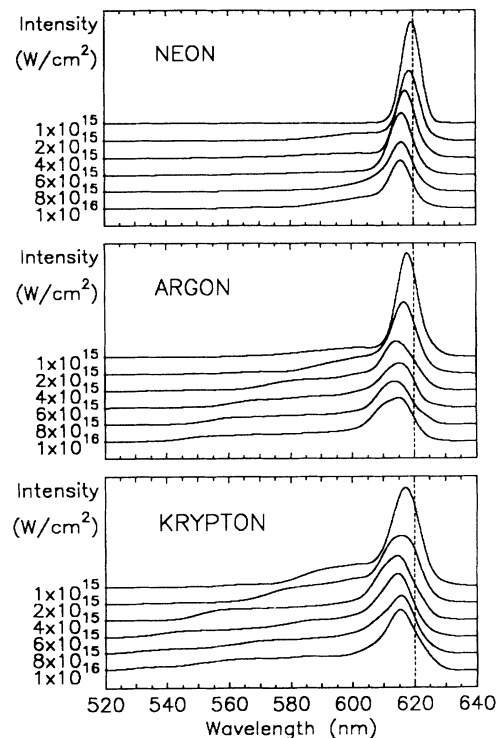

FIG. 8. Averaged spectra, including collisional ionization, for $f/5$ focusing of a 620-nm, 100-fs FWHM pulse in 5-atm Ne, Ar, and Kr.
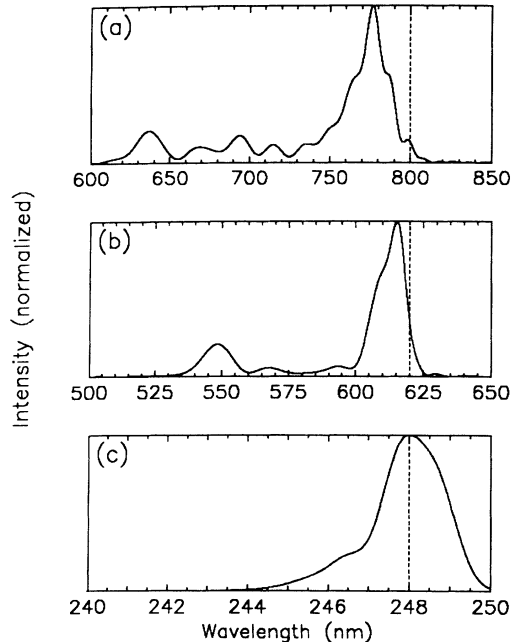
FIG. 9. Transmitted pulse spectra, including collisional ionization, for a 100-fs FWHM pulse at a peak intensity of 10^{16} W/cm^2, Ar at 5 atm, and an interaction length equal to the confocal parameter for $f/5$ focusing. Laser wavelength (a) 800 nm, (b) 620 nm, (c) 248 nm.

remains at the original wavelength. It is also worth noting the much smaller extent of the blueshift, a consequence of the λ_0^3 dependence. It would seem that a much higher intensity or much larger interaction length would be needed before this mechanism could produce a useful source of broadband vacuum ultraviolet radiation. In contrast, at 800 nm the quiver energy is around 600 eV at 10^{16} W/cm^2, and here collisional ionization is almost equal in importance with OFI. The spectrum is much broader and the main peak is shifted considerably from the original wavelength.

VI. DISCUSSION

The simulated spectra in Fig. 8 correspond quite closely to the experimental results of Ref. [8], except that the intensity required in the simulations to match the extent of the blueshifted shoulder is significantly (a factor of 5–10) lower than the experimentally estimated intensity. This is in contrast with the simpler homogeneous plasma model used in Ref. [8], which showed agreement with the experimental results at the "correct" experimental intensity. There are a number of possible reasons for the discrepancy observed in the present case, including uncertainties over the intensity distribution in the focal region and approximations over ionization rates and laser pulse shape, but the most important factor is defocusing in the plasma caused by the extremely large electron density gradients near the focal point.

We will use the case of krypton at 5 atm and a vacuum (i.e., plasma-free) intensity of 10^{16} W/cm^2 as an example,

to show the necessity of taking defocusing into account. If defocusing effects were ignored, and an actual intensity of 10^{16} W/cm^2 assumed, then the degree of ionization calculated from our model would be 6.0. The electron density at the focal point would thus be 7.5×10^{20} cm^{-3}, and the refractive index would be reduced from unity to 0.861. The phase change, ϕ, over a distance equal to the confocal parameter, would be given by $\phi = (2\pi/\lambda_0)z_c\Delta n \simeq 18\pi$. Considering that the phase change required for an increase in divergence of one diffraction-limited beam divergence is $\phi = \pi$, there would obviously be a severe modification to the spatial properties of the beam, and the intensity would be much reduced from its vacuum value.

Through tunneling ionization, the degree of ionization in the gas depends on the actual focused intensity, and as a result of defocusing, the intensity also depends on the degree of ionization. For any given set of conditions, there will be some particular intensity, reduced from the vacuum intensity, at which these two effects balance. In the case of krypton at 5 atm, the present model suggests that this occurs at a defocused intensity of around 1×10^{15} W/cm^2. A similar conclusion is reached for argon, but for neon, where the higher ionization potentials reduce the degree of ionization, the defocusing is seen to be somewhat less severe.

Given that a certain degree of defocusing is simply unavoidable, it would appear that the simple model used in Ref. [8] and based on Eq. (8), although presenting a qualitatively accurate picture of the physical origin of the blueshifting, underestimates the magnitude of the blueshift. This should not be surprising, as by assuming that different regions of the plasma contribute independently to an overall shift, the simple model ignores the coherent aspect of the propagation.

Apart from the complicated defocusing effects, quantitative predictions from the present model are ultimately limited by the accuracy of the rate calculations, both for OFI and collisional ionization. The collisional ionization rates we have used assume that atoms and ions are in their ground state, and it has been suggested by Lotz [16] that excited-state populations may increase the effective impact ionization cross section by as much as an order of magnitude. Excited-state populations would also affect OFI, however, and this would have a large effect on the transmitted pulse spectrum, increasing the extent of the blue shoulder. It is difficult to make a quantitative estimate of this effect and, in any case, there is no evidence from the present work or from other experimental studies on highly charged ion production [11] that excited states play an important role.

By developing a more detailed physical model for blueshifting, it was hoped that experiments would be able provide a useful comparative test of various theoretical calculations of optical field-induced ionization, an alternative to ion-counting experiments such as those of Augst et al. [11] and Gibson, Luk, and Rhodes [17]. The importance of spatial effects, however, means that it is difficult to separate effects due to defocusing from effects due to possible inaccuracies in the ionization rate calculations. To clarify the situation, some additional informa-

tion is required, perhaps from a higher-dimensional model (which would remove many of the assumptions inherent in our 1D treatment), or from an independent experimental measurement of the defocusing or the peak degree of ionization.

In conclusion, we have shown that a 1D propagation-ionization model can be used to predict the transmitted spectrum of an intense femtosecond laser pulse after passage through an atmospheric-density noble gas. For an incident wavelength of 620 nm, the spectrum shows a mean peak blueshifted by a few nanometers, due primarily to collisional ionization, and an intensity-dependent blue shoulder which extends over 10–100 nm, due mainly to OFI. The extent of the blueshifted shoulder depends on the ionization potentials of the gas, being significantly larger in krypton and argon than in neon. All these features are in quantitative agreement with recent experiments of Wood, Siders, and Downer [8], however, defocusing appears to decrease the peak intensity considerably below that expected with no plasma formation. For the purposes of testing ionization rate calculations, a simpler experimental situation to analyze would involve a shorter laser wavelength, reducing the quiver energy and hence the collisional ionization rate, and larger f-number optics, reducing the effect of plasma defocusing.

[1] For a comprehensive review, see *The Supercontinuum Laser Source,* edited by R. R. Alfano (Springer-Verlag, Berlin, 1989).

[2] N. Bloembergen, Opt. Commun. **8**, 285 (1973).

[3] E. Yablonovitch, Phys. Rev. A **10**, 1888 (1974).

[4] P. B. Corkum, IEEE J. Quantum Electron. **21**, 216 (1985).

[5] W. M. Wood, G. Focht, and M. C. Downer, Opt. Lett. **13**, 984 (1988).

[6] M. C. Downer, W. M. Wood, and J. I. Trisnadi, Phys. Rev. Lett. **65**, 2832 (1990).

[7] M. C. Downer *et al.,* in *Proceedings of the Tenth International Conference on Spectral Line Shapes,* edited by L. Frommhold and J. W. Keto, AIP Conf. Proc. No. 216 (AIP, New York, 1990).

[8] W. M. Wood, C. W. Siders, and M. C. Downer, Phys. Rev. Lett. **67**, 3523 (1991).

[9] M. V. Ammosov, N. B. Delone, and V. P. Krainov, Zh. Eksp. Teor. Fiz. **91**, 2008 (1986) [Sov. Phys.—JETP **64**, 1191 (1987)].

[10] A. M. Perelomov, V. S. Popov, and M. V. Terentev, Zh. Eksp. Teor. Fiz. **50**, 1393 (1966) [Sov. Phys.—JETP **23**, 924 (1966)].

[11] S. Augst, D. D. Meyerhofer, D. Strickland, and S. L. Chin, J. Opt. Soc. Am. B **8**, 858 (1991).

[12] This intensity scaling factor was found to be 1.8 for neon, 1.7 for argon, and 1.2 for krypton. The electric field needs to be divided by the square root of the appropriate factor before being used in the ADK expression.

[13] S. C. Rae and K. Burnett, Phys. Rev. A (to be published).

[14] A compilation of experimental data on electron-impact ionization cross sections for a wide range of elements has been published by H. Tawara and T. Kato, At. Data Nucl. Data Tables **36**, 167 (1987). For our calculation, we use a best-fit curve to the average of these experimental data.

[15] M. C. Downer (private communication).

[16] W. Lotz, Z. Phys. **216**, 241 (1968).

[17] G. Gibson, T. S. Luk, and C. K. Rhodes, Phys. Rev. A **41**, 5049 (1990).